An allosteric modulator binds to a conformational hub in the β₂ adrenergic receptor

Xiangyu Liu [1,2,10], Jonas Kaindl [3,10], Magdalena Korczynska[4], Anne Stößel[3], Daniela Dengler[3], Markus Stanek[3], Harald Hübner[3], Mary J. Clark [5], Jake Mahoney[5], Rachel Ann Matt [6], Xinyu Xu[2,7], Kunio Hirata [8,9], Brian K. Shoichet [4], Roger K. Sunahara [5 ✉], Brian K. Kobilka [2,6,7 ✉] and Peter Gmeiner [3 ✉]

---

[1]School of Pharmaceutical Sciences, Tsinghua University, Beijing, China. [2]Beijing Advanced Innovation Center for Structural Biology, Tsinghua University, Beijing, China. [3]Department of Chemistry and Pharmacy, Medicinal Chemistry, Friedrich-Alexander University Erlangen-Nürnberg, Erlangen, Germany. [4]Department of Pharmaceutical Chemistry, University of California, San Francisco, CA, USA. [5]Department of Pharmacology, University of California San Diego School of Medicine, La Jolla, CA, USA. [6]Department of Molecular and Cellular Physiology, Stanford University School of Medicine, Stanford, CA, USA. [7]School of Medicine, Tsinghua University, Beijing, China. [8]Advanced Photon Technology Division, Research Infrastructure Group, SR Life Science Instrumentation Unit, RIKEN/SPring-8 Center Sayo-gun, Hyogo, Japan. [9]Precursory Research for Embryonic Science and Technology, Japan Science and Technology Agency, Saitama, Japan. [10]These authors contributed equally: Xiangyu Liu, Jonas Kaindl. ✉e-mail: rsunahara@ucsd.edu; kobilka@stanford.edu; peter.gmeiner@fau.de

Supplementary Table 1. Data collection and refinement statistics (molecular replacement).

	Native[a]	Anomalous (Br)[b]
Data collection		
Space group	$P2_12_12_1$	$P2_12_12_1$
Cell dimensions		
a, b, c (Å)	40.46, 75.71, 173.41	40.46, 75.71, 173.41
α, β, γ (°)	90.00, 90.00, 90.00	90.00, 90.00, 90.00
Resolution (Å)	49.4-3.1 (3.2-3.1) *	50-4.0 (4.1-4.0)
R_{sym} or R_{merge}	0.21 (1.11)	0.32 (1.80)
$I / \sigma I$	8.46 (1.27)	16.07 (4.20)
Completeness (%)	99.1 (98.2)	99.9 (99.8)
Redundancy	13.3 (9.7)	54.6 (56.0)
Refinement		
Resolution (Å)	20-3.1	
No. reflections (test set)	10122 (999)	
R_{work} / R_{free}	0.251/0.277	
No. atoms		
Protein	3523	
Alprenolol	18	
AS408	19	
Others (Lipids, ions, water)	56	
B-factors		
Receptor	84.0	
T4 lysozyme	102.4	
Alprenolol	73.2	
AS408	70.4	
Others (Lipids, ions, water)	100.2	
R.m.s. deviations		
Bond lengths (Å)	0.008	
Bond angles (°)	0.750	

[a] X-ray diffraction data from 81 LCP crystals was merged to get the native dataset.
[b] X-ray diffraction data from 284 LCP crystals was merged to get the anomalous dataset.
*Values in parentheses are for highest-resolution shell.

Supplementary Table 2. Allosteric values describing the effects of AS408 in norepinephrine-stimulated signaling assays.

Complete Operational Model of Allostery*	[^{35}S]GTPγS Binding	cAMP Accumulation	β-arrestin Recruitment
Best-fit values			
Log (K_A)	-5.7 +/- 0.5	-4.9 +/- 0.1	-4.6 +/- 0.1
Log (K_B)	-6.8 +/- 0.1	-5.9 +/- 0.1	-5.8 +/- 0.1
Log (α)	-0.7 +/- 0.5	-0.1 +/- 0.1	-0.2 +/- 0.1

* Allostery values for AS408 on norepinephrine-stimulated [^{35}S]GTPγS binding, cAMP accumulation and β-arrestin recruitment were determined using the complete operational model of allostery (Prism, GraphPad, CA). Maximal values were held constant within each assay and $τ_β$ and β-values were fixed at ~0 since AS408 is a NAM and has no agonist efficacy, respectively.

Data from norepinephrine dose-response curves in the presence of varying concentrations of AS408 (1, 3, 10 and 30 μM) for [^{35}S]GTPγS binding, cAMP accumulation and β-arrestin recruitment were fitted using the complete operational model of allostery using GraphPad Prism 6.0 (GraphPad, San Diego, CA). Basal and maximal responses were fixed, according to the specific assays, and $τ_β$- and β-values were fixed at zero with the assumption that AS408 is a NAM for agonists and an inverse agonist in cAMP and GTPγS binding assays.

Supplementary Table 3. Pharmacological characterization of AS408 by radioligand binding analysis to β_2AR (wt) and E122$^{3.41}$ mutants.

β_2AR Alone	β_2AR (wt) Log(Kd/Ki), M	N	Fold Shift	β_2AR (E122Q) Log(Kd/Ki), M	N	Fold Shift	β_2AR (E122L) Log(Kd/Ki), M	N	Fold Shift	β_2AR (E122R) Log(Kd/Ki), M	N	Fold Shift
Kd [³H]DHAP	-9.42+/-0.46	3		-9.61+/-0.73	3		-9.61+/-0.58	3		-9.05+/-0.32	3	
Kd [³H]DHAP + 30 µM AS408	-9.74+/-0.70	3		-9.46+/-0.38	3		-8.75+/-0.45*	3		-9.14+/-0.24	3	
Fold Kd AS408/DMSO			0.5			1.4			7.2			0.8
Ki NE	-5.75+/-0.07	3		-5.89+/-0.04**[1]	3		-4.95+/-0.03**[1]	3		-4.17+/-0.06**[1]	3	
Ki NE + 30 µM AS408	-5.29+/-0.12*	3		-5.47+/-0.06**	3		-4.61+/-0.06*	3		-4.20+/-0.04	3	
Fold Ki AS408/DMSO			3.2			2.6			2.2			0.9
Ki EPI	-6.97+/-0.05	4		-7.07+/-0.05**[1]	3		-6.33+/-0.04**[1]	3		-4.94+/-0.06**[1]	3	
Ki EPI + 30 µM AS408	-6.45+/-0.09**	4		-6.69+/-0.09**	3		-5.47+/-0.05**	3		-4.98+/-0.07	3	
Fold Ki AS408/DMSO			3.3			2.4			7.2			0.9
Ki SALB	-6.12+/-0.02	3		-6.46+/-0.05**[1]	3		-5.97+/-0.02**[1]	3		-5.29+/-0.04**[1]	3	
Ki SALB + 30 µM AS408	-5.70+/-0.03**	3		-6.05+/-0.04**	3		-5.47+/-0.04**	3		-5.25+/-0.05	3	
Fold Ki AS408/DMSO			2.6			2.6			3.2			1.1
Ki ICI	-9.66+/-0.06	3		-9.57+/-0.02**[1]	3		-9.56+/-0.02**[1]	3		-9.88+/-0.03**[1]	3	
Ki ICI + 30 µM AS408	-10.02+/-0.02**	3		-9.66+/-0.03*	3		-8.84+/-0.05**	3		-9.78+/-0.04*	3	
Fold Ki AS408/DMSO			0.4			0.8			5.3			1.3

β_2AR +Gs$\alpha\beta\gamma$	β_2AR (wt) Log (Ki), M	N	Fraction High (%)	Fold shift	β_2AR (E122Q) Log (Ki), M	N	Fraction High (%)	Fold shift	β_2AR (E122L) Log (Ki), M	N	Fraction High (%)	Fold shift	β_2AR (E122R) Log (Ki), M	N	Fraction High (%)	Fold shift
Khigh NE	-7.87+/-0.12	4	37		-8.13+/-0.23	3	31		-7.64+/-0.32	4	18*[1]		-7.18+/-0.13**[1]	4	43	
Khigh NE + 30 µM AS408	-7.67+/-0.19	4	32		-7.81+/-0.20	3	24		-6.60+/-0.43*	4	16		-7.34+/-0.12	4	44	
Fold Khigh AS408/DMSO				1.3				2.1				11				0.7
Klow NE	-5.52+/-0.07	4			-5.94+/-0.10*[1]	3			-5.25+/-0.07*[1]	4			-4.63+/-0.10**[1]	4		
Klow NE + 30 µM AS408	-4.96+/-0.09**	4			-5.59+/-0.07**	3			-5.01+/-0.14	4			-4.58+/-0.10	4		
Fold Klow AS408/DMSO				3.6				2.2				2.0				1.1
Khigh EPI	-9.18+/-0.08	8	39		-9.15+/-0.22	4	26		-8.21+/-0.16*[1]	4	30		-8.07+/-0.12**[1]	4	51*[1]	
Khigh EPI + 30 µM AS408	-8.6+/-0.11**	8	32*		-8.88+/-0.23	4	23		-7.09+/-0.30	4	43		-8.04+/-0.11	4	49	
Fold Khigh AS408/DMSO				3.8				1.9				13				1.1
Klow EPI	-6.64+/-0.05	8			-7.08+/-0.08	4			-6.20+/-0.07**[1]	4			-5.47+/-0.14**[1]	4		
Klow EPI + 30 µM AS408	-5.87+/-0.06**	8			-6.85+/-0.07*	4			-5.80+/-0.24	4			-5.53+/-0.11	4		
Fold Klow AS408/DMSO				5.8				1.7				2.5				0.8

*p<0.05 vs DMSO, **p<0.001 vs DMSO, *[1]p<0.05 vs β_2AR(wt), **[1]p<0.001 vs β_2AR(wt)

Membranes prepared from *Sf9* cells infected with baculoviruses expressing β_2AR (wt) or E122 mutants in the absence or presence of co-expressed Gs heterotrimer were assessed by radioligand binding with [³H]DHAP. Inhibition of [³H]DHAP binding by full agonists epinephrine and norepinephrine and inverse agonist ICI-118,551 was measure in the absence or presence of 30 µM AS408. K_i were determined using GraphPad Prism 6.0 (GraphPad, San Diego, CA) using the K_d of [³H]DHAP specific for β_2AR (wt) and each mutant, according to the Cheng-Prusoff equation[1]. Values for high affinity agonist site (K_{high}) and low affinity site (K_{low}) from membranes prepared from β_2AR (wt) or mutants co-infected with Gs heterotrimer were determined by non-linear regression fitting (2-site) using K_d values of [³H]DHAP, as above (GraphPad, San Diego, CA). The statistical analysis of the effect of AS408 in the competition assays (K_i) was performed using the extra sum-of-squares F-test based on the ligand binding data fit to a logistics equation above using Prism™. Sample size (N) is included in the table and the significant differences are demarcated with asterisks with the p-values included in table footnote.

1   Cheng, Y. & Prusoff, W. H. Relationship between the inhibition constant (K1) and the concentration of inhibitor which causes 50 per cent inhibition (I50) of an enzymatic reaction. *Biochem Pharmacol* **22**, 3099-3108 (1973).

Supplementary Table 4. Allosteric values for AS408 on norepinephrine-stimulated [^{35}S]GTPγS binding assay for the β$_2$AR and β$_1$AR.

Complete Operational Model of Allostery*	β$_2$AR-wt	β$_1$AR-NE NE
Best-fit values		
Log (K$_A$)	-5.7 +/- 0.5	-5.7 +/- 0.1
Log (K$_B$)	-6.8 +/- 0.1	-5.6 +/- 0.1
Log (α)	-0.7 +/- 0.5	-0.4 +/- 0.2

* Allostery values for AS408 on norepinephrine-stimulated [^{35}S]GTPγS binding for β$_2$AR and β$_1$AR were determined using the complete operational model of allostery (Prism, GraphPad, CA). Maximal values were held constant within each assay and τ$_β$ and β-values were fixed at ~0 since AS408 is a NAM and has no agonist efficacy, respectively.

Data were fitted using the complete operational model of allostery using GraphPad Prism 6.0 (GraphPad, San Diego, CA). Maximal values were held constant and τ$_β$- and β-values were fixed at ~ 0 since AS408 is a NAM and has no agonist efficacy, respectively.

Supplementary Table 5. Analysis of the inhibitory effects of AS408 on agonist stimulated β-arrestin recruitment assay of the μ-opioid receptor and dopamine D2 receptor.

	μOR DAMGO	DRD2 quinpriole
Null hypothesis	Gaddum/Schild EC_{50} shift	Gaddum/Schild EC_{50} shift
Alternative hypothesis	Allosteric EC_{50} shift	Allosteric EC_{50} shift
Best fit (p < 0.05)	Gaddum/Schild EC_{50} shift	Gaddum/Schild EC_{50} shift
Schild Slope	1.7 +/- 0.1	1.1 +/- 0.1
Log(EC_{50})	-5.9 +/- 0.1	-7.2 +/- 0.1
Log (K_B)	-5.0 +/- 0.1	-4.7 +/- 0.1

* The inhibitory effects of AS408 on agonist-stimulated β-arrestin recruitment for the μ-opioid receptor (μOR) and dopamine D2 receptor (DRD2) by DAMGO or quinpirole, respectively, were analyzed by the Allosteric Ternary Complex Model[15] or by Gaddum/Schild analysis[15] (Prism, GraphPad, CA). An F-fest was performed to determine which model best fits the data (p<0.05) and suggests that the inhibitory effects of AS408 would be best approximated by Schild analysis. The variables for the model comparison were shared among all data sets for each receptor.

The inhibitory effects of AS408 on agonist-stimulated β-arrestin recruitment for the μ-opioid receptor (μOR) and dopamine D2 receptor (DRD2) by DAMGO or quinpirole, respectively, were analyzed by the Allosteric Ternary Complex Model or by Gaddum/Schild analysis[2] using GraphPad Prism 6.0 (GraphPad, San Diego, CA). An F-fest was performed to determine which model best fits the data (p < 0.05) and suggests that the inhibitory effects of AS408 would be best approximated by Schild analysis. The variables for the model comparison were shared among all data sets for each receptor. The sample size of the experiment is described in Supplementary Fig. 6.

2   Christopoulos, A. & Kenakin, T. G protein-coupled receptor allosterism and complexing. *Pharmacol Rev* **54**, 323-374, doi:10.1124/pr.54.2.323 (2002).
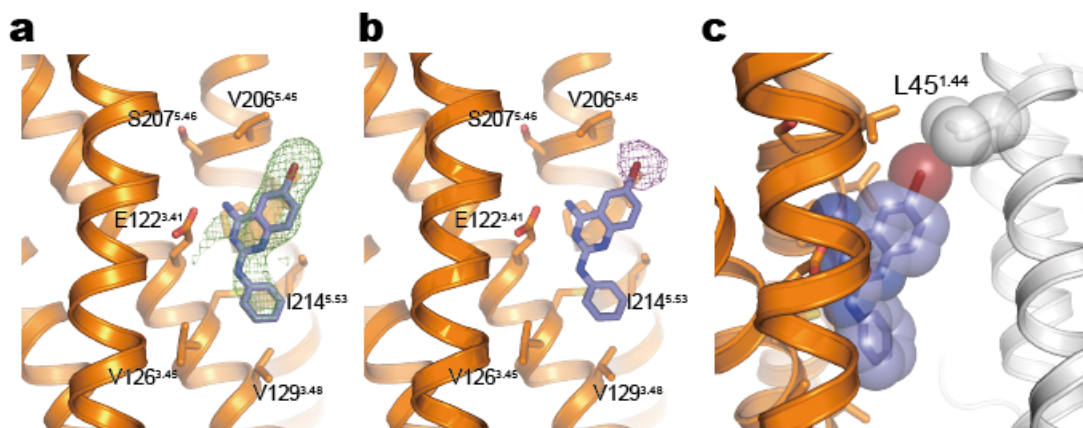
Supplementary Figure 1. Structure of the AS408 binding site. (**a**) Fo-Fc simulated annealing omit map (green, contoured at $2.3\,\sigma$) reveals the binding site of AS408 in the AS408-β_2AR complex in the presence of alprenolol. (**b**) Anomalous signal (purple, contoured at $4.0\,\sigma$) of the bromine atom at C_6 of AS408 yields a unique density corresponding to the AS408 model in (**a**). (**c**) The bromine moiety of AS408 forms a crystal contact with L45$^{1.44}$ of a neighboring β_2AR in the crystal lattice.
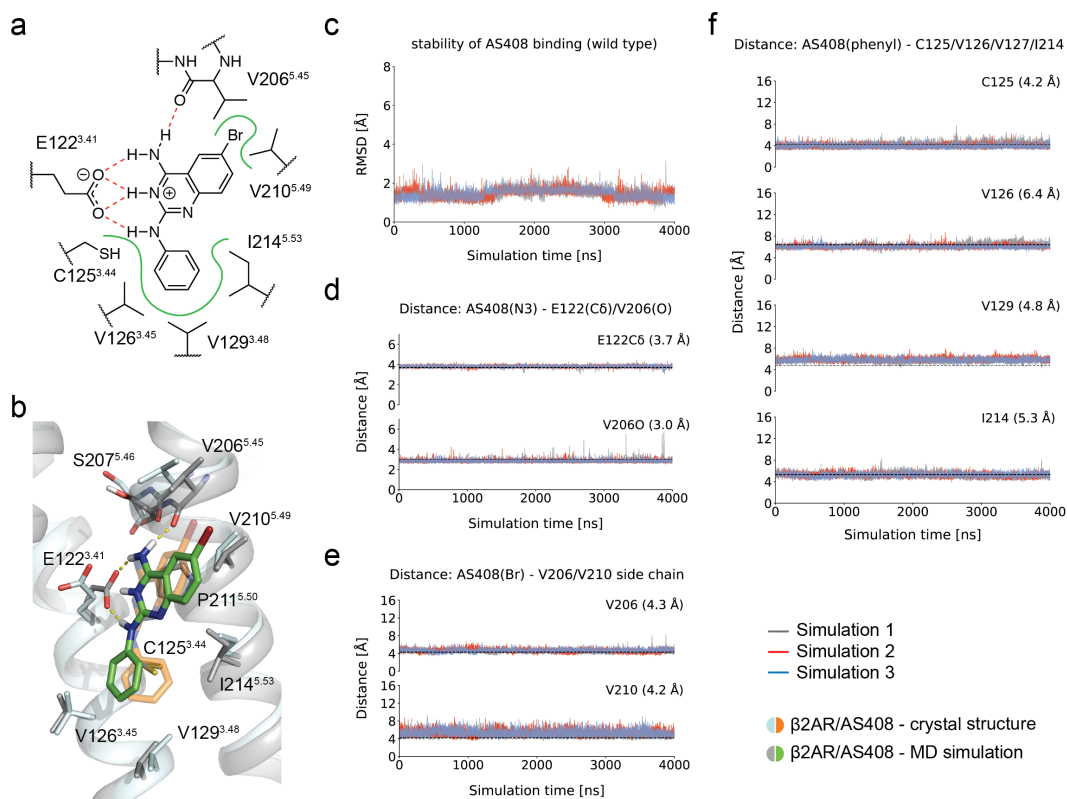
Supplementary Figure 2. Molecular dynamics (MD) simulations of AS408 at the β₂AR in complex with alprenolol. (**a**) Interaction pattern of AS408 protonated at position 3 when bound to β₂AR. Simulations with AS408 protonated at other positions (N1 or NH₂) or in the neutral state resulted in less stable interactions with the receptor. (**b**) Representative, energy minimized snapshot of the MD simulation of AS408 bound to β₂AR superimposed with the crystal structure of inactive β₂AR in complex with alprenolol and AS408. (**c**) Rmsd of AS408 showing that AS408 maintains a binding mode comparable to its crystallographic pose. (**d**) The primary amine of AS408 stays within hydrogen bonding distance of the carboxylate of E122$^{3.41}$ and the carbonyl oxygen of V206$^{5.45}$. (**e**) The bromo substituent of AS408 maintains its van der Waals interactions to the side chains of V206$^{5.45}$ and V210$^{5.49}$. Binding doesn't require a second β₂AR protomer. (**f**) The unsubstituted phenyl ring of AS408 maintains its position between the side chains of C125$^{3.44}$, V126$^{3.45}$, V129$^{3.48}$ and I214$^{5.53}$. (**d – f**) Dashed lines show the distance observed in the crystal structure. The exact values are written in brackets.
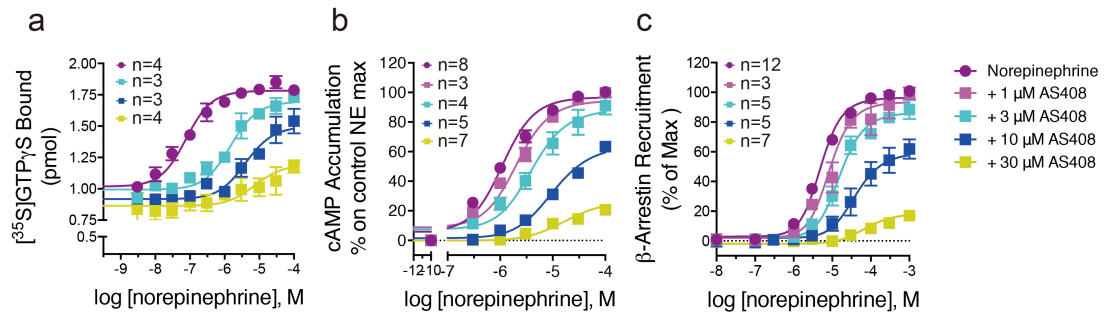
Supplementary Figure 3. The allosteric of effects of AS408 on norepinephrine-stimulated signaling assays. Norepinephrine dose-response curves in the presence of varying concentrations of AS408 (demarcated) for (**a**) [^{35}S]GTPγS binding, (**b**) cAMP accumulation and (**c**) β-arrestin recruitment. Data are similar to those data reported in Figures 1e and f and Figures 5a, d and h but fitted using the complete operational model of allostery using GraphPad Prism 6.0 (GraphPad, San Diego, CA). Basal and maximal responses were fixed, according to the specific assays, and τ$_β$- and β-values were fixed at zero with the assumption that AS408 is a NAM for agonists and an inverse agonist in cAMP and GTPγS binding assays. Data are given as mean ± SEM of 3 – 12 experiments performed in duplicate. The sample size (n) is labeled in the figure.
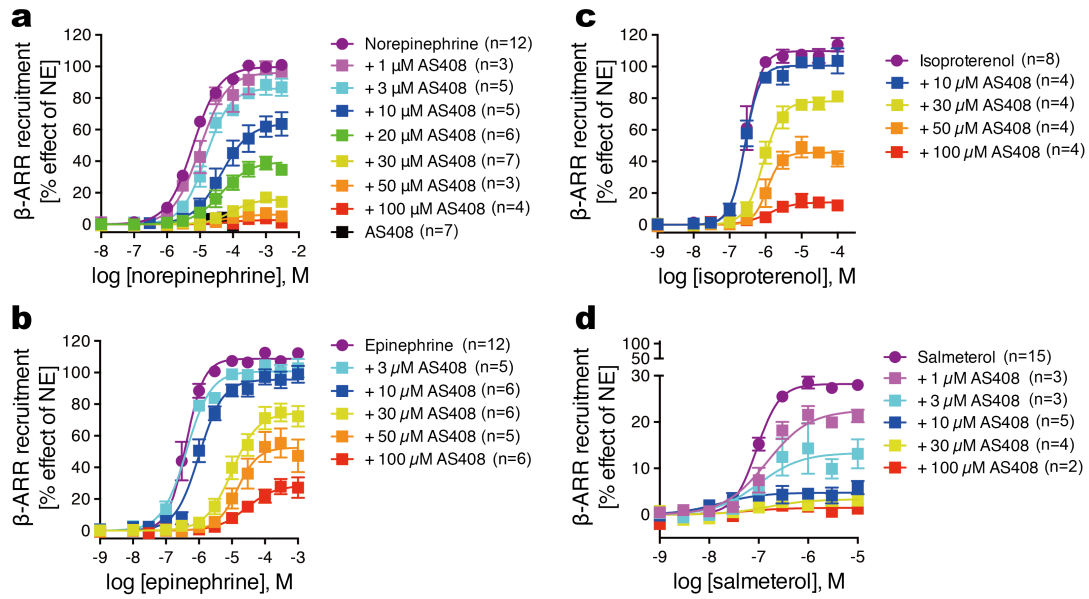
Supplementary Figure 4. Negative allosteric activity of AS408 on agonist-mediated β-arrestin 2 recruitment to β₂AR. (**a – d**) Varying concentration of AS408 on dose response curves for full agonists (**a**) norepinephrine, (**b**) epinephrine (**c**) isoproterenol, or (**d**) partial agonist salmeterol. Data are derived from 2 – 15 experiments performed in duplicate and are given as mean ± SEM if n ≥ 3, or as mean if n = 2. The sample size (n) is labeled in the figure. Note AS408 (black symbols) appears to have no positive intrinsic effect on β-arrestin recruitment on its own.
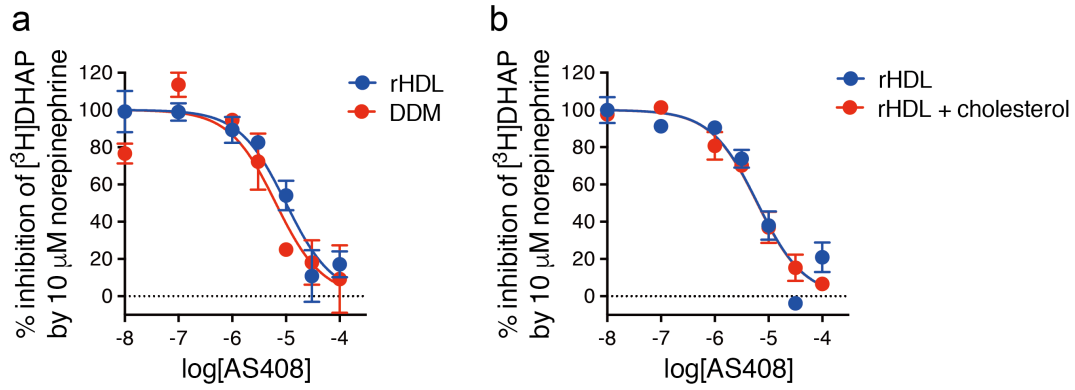
Supplementary Figure 5. AS408 reverses norepinephrine inhibition of [³H]DHAP binding to β₂AR in detergent micelles or in lipid. AS408 reversed 10 μM norepinephrine inhibition of [³H]DHAP binding to the β₂AR in (**a**) dodecylmaltoside (DDM) micelles or reconstituted in high density lipoprotein particles (rHDL or nanodiscs) (log(EC50) ~ -5.2 ± 0.23 and -5.0 ± 0.17, respectively), or (**b**) in rHDL in the absence or presence of cholesterol (log(EC50) ~ -5.2 ± 0.15 and -5.2 ± 0.10, respectively). Data are given as mean ± SEM of 3 independent measurements.
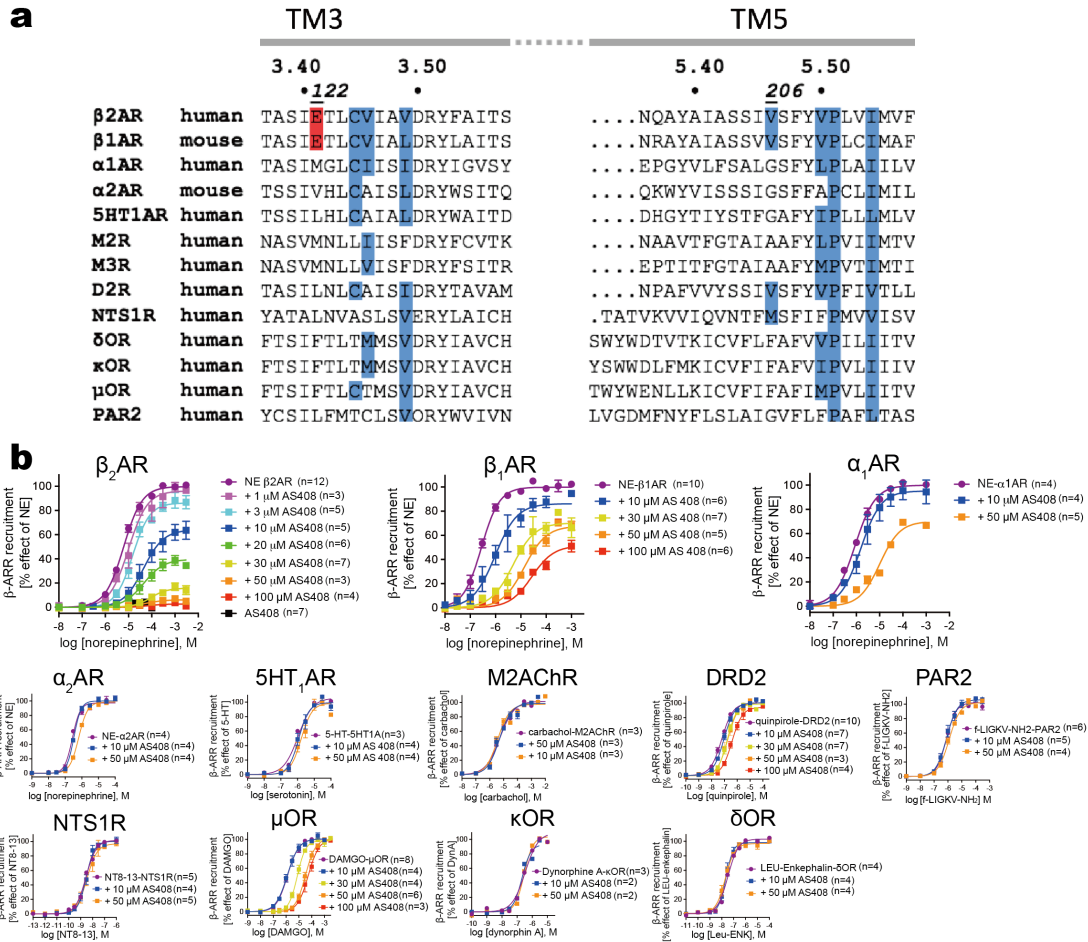
Supplementary Figure 6. β-adrenergic receptor selectivity of AS408. (a) Sequence alignment of residues in TM3 and TM5 involved in AS408 binding from various family A GPCRs. Conserved residues are highlighted in blue whereas β-adrenergic receptor-specific E122$^{3.41}$ is shaded in red. (**b**) AS408 preferentially modulates agonist-stimulated β-arrestin 2 recruitment on β$_2$AR and β$_1$AR compared to other family A GPCRs. Data are derived from 2 – 12 experiments done in duplicate and are given as mean ± SEM if n ≥ 3, or as mean if n = 2.; the sample size (n) is labeled in the figure.
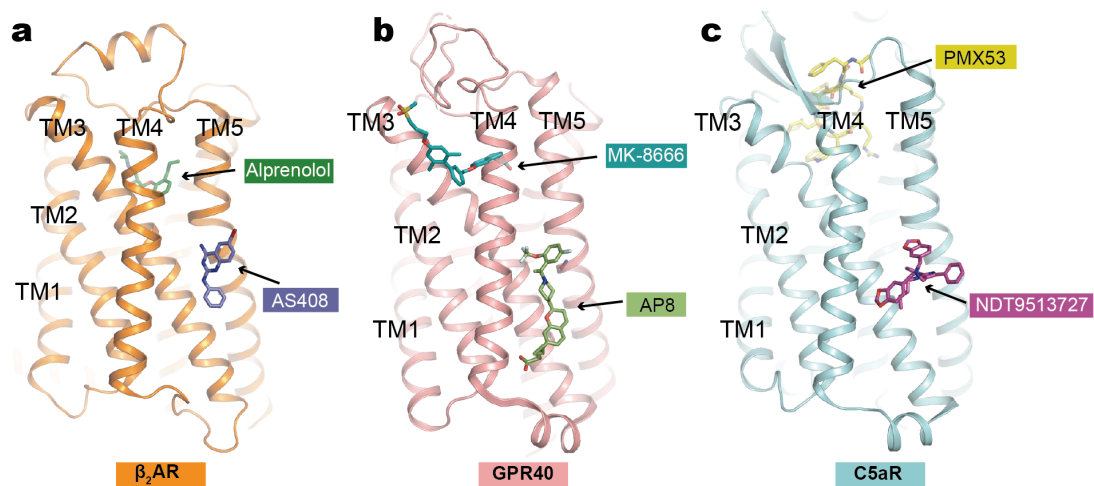
Supplementary Figure 7. Binding of allosteric modulators to the lipid-facing allosteric pocket formed between TM3 and TM5 in GPCRs. Structure of (**a**) AS408 bound to β_2AR with respect to orthosteric ligand alprenolol in comparison to (**b**) positive allosteric modulator (AP8) bound to free-fatty acid receptor 1 (FFAR1 or GPR40), in the presence of orthosteric partial agonist MK-8666 (PDB: 5TZY) and (**c**) negative allosteric modulator (NDT9513727) bound to complement C5a receptor in the presence of orthosteric antagonist PMX53 (PDB: 6C1Q).
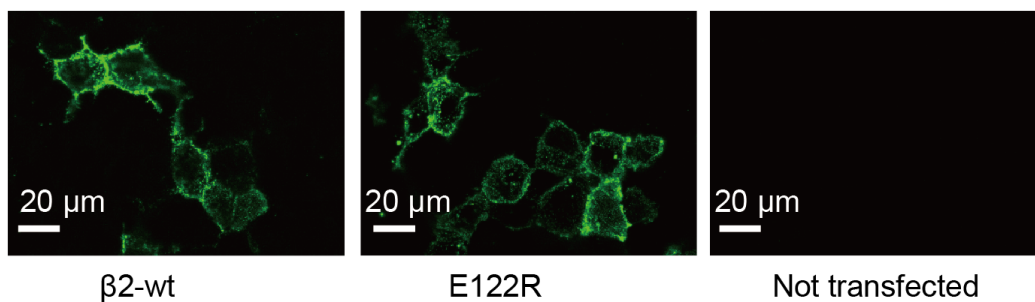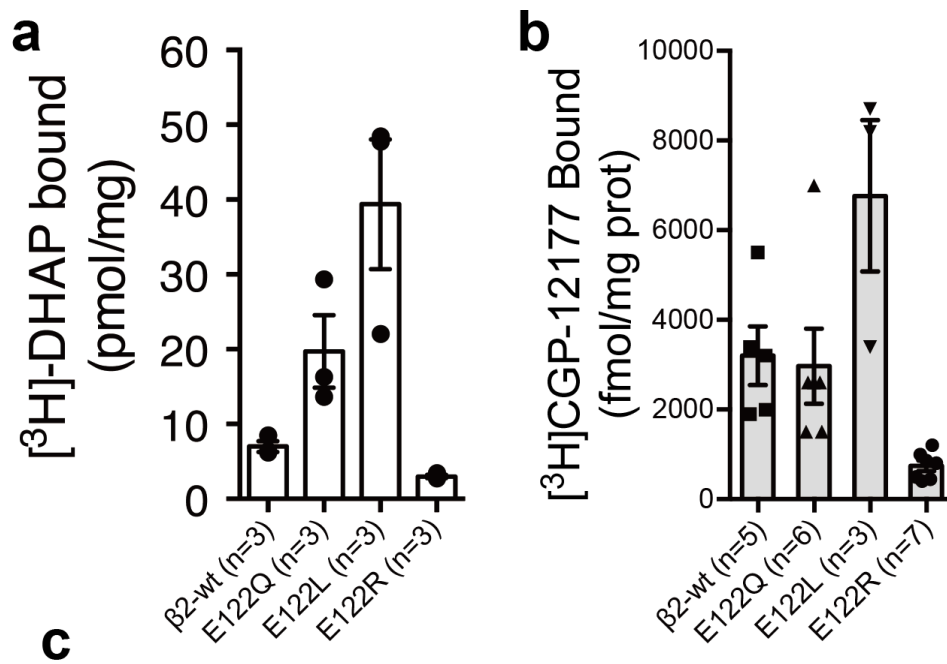
Supplementary Figure 8. Expression of E122x mutants β_2AR in HEK cells. (**a**) [^{3}H]DHAP binding to E122 mutants of β_2AR expressed in HEK293 cells, or (**b**) measured with weak partial agonist binding ([^{3}H]CGP12177). Data are given as mean ± SEM of 3 - 7 independent measurements. The sample size (n) is labeled in the figure. (**c**), Cell surface expression of wt and E122R β_2AR measured with immunofluorescence confocal microscopy. Approximately 20 cells in each of 3 different regions of interest on the coverslips were examined with similar results and the representative images were shown in the figure.
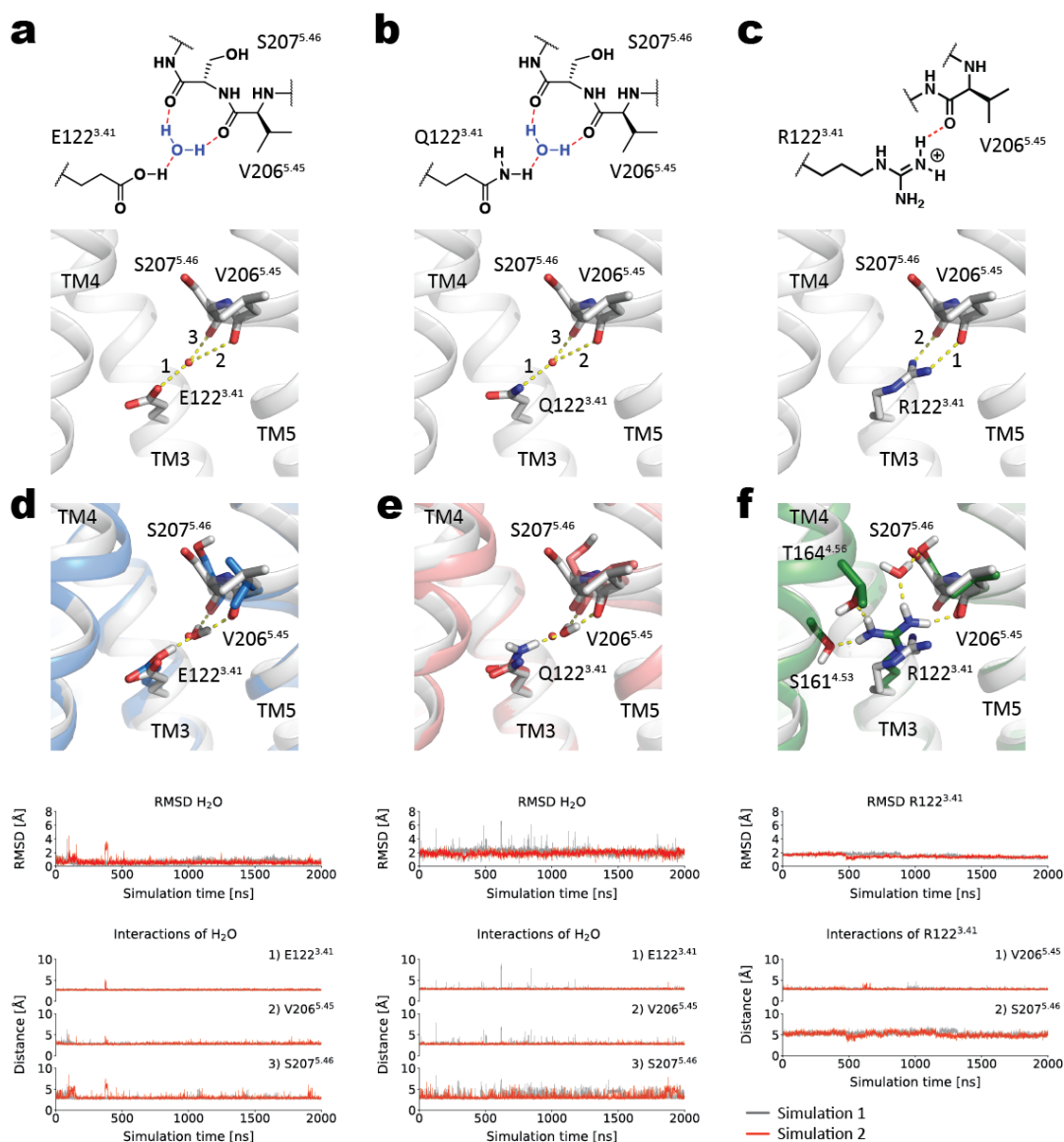
Supplementary Figure 9. Mutation of E122$^{3.41}$ influences stability of hydrogen bond network, observed in molecular dynamics (MD) simulations. Figures (**a** – **c**) illustrate the networks involving position 122$^{3.41}$ at β$_2$AR wild type (E122$^{3.41}$) and putative interactions of the mutants Q122$^{3.41}$ and R122$^{3.41}$. These networks include E, Q or R122$^{3.41}$, a mediating water, V206$^{5.45}$ and S207$^{5.46}$. The R122$^{3.41}$ mutant was modeled to directly interact with V206$^{5.45}$ and S207$^{5.46}$ excluding the water molecule found in the wild type crystal structure (PDB: 2RH1). The interactions to be analyzed are marked by "1", "2" and "3". (**d** – **f**) MD simulations. (**d**, **e**) The polar network stays intact for the simulations of wild type β$_2$AR (E122$^{3.41}$) and its mutant Q122$^{3.41}$. This includes a weaker interaction between the mediating water molecule and the backbone oxygen of Ser207$^{5.46}$ for the Q122$^{3.41}$ mutant, observable in higher rmsd levels for the water molecule and a less frequent interaction to the backbone oxygen of Ser207$^{5.46}$ (97% for E122$^{3.41}$, 85% for Q122$^{3.41}$). Representative snapshots of the MD simulations of β$_2$AR wild type and the Q122$^{3.41}$ mutant superimposed with the β$_2$AR crystal structure or the modeled Q122$^{3.41}$ mutant are shown in blue and grey or red and grey, respectively. (**f**) R122$^{3.41}$ does not maintain the full polar network, as its side chain rotates away from Ser207$^{5.46}$ but maintains a stable interaction to V206$^{5.45}$.

A representative snapshot of the R122$^{3.41}$ mutant simulations superimposed with the modeled R122$^{3.41}$ mutant is shown in green and grey, respectively.
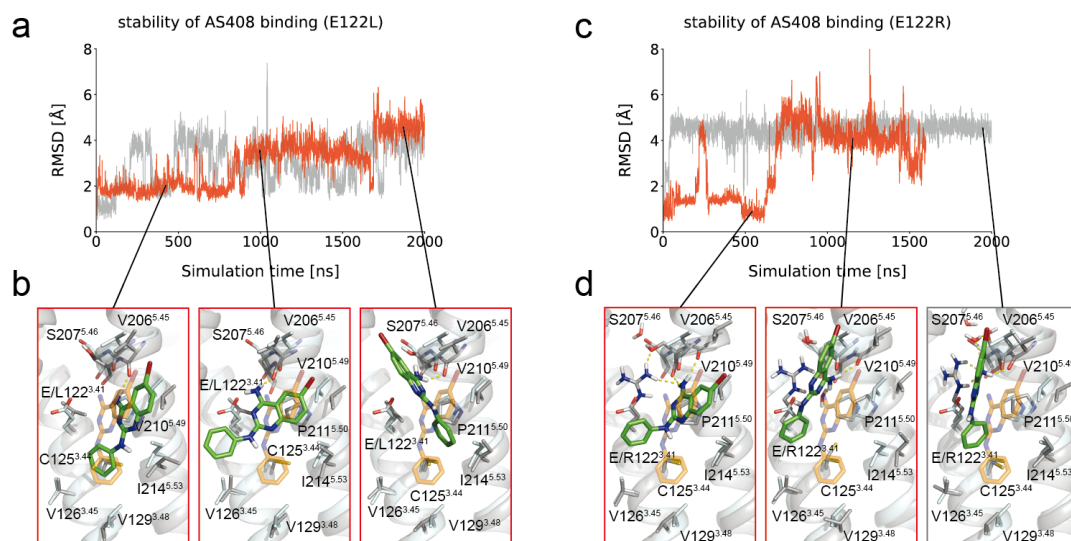
Supplementary Figure 10. Molecular dynamics (MD) simulations of AS408 at the β₂AR E122X mutations. (**a, c**) Rmsd traces for simulations of AS408 at E122L and E122R mutant. (**a**) In the simulations of neutral AS408 at the E122L mutant, AS408 remains at the allosteric site adopting several conformations and maintains a hydrogen bond of AS408 to the backbone oxygen of V206$^{5.45}$. The significantly reduced stability suggests a less stable interaction with the mutant compared to β₂AR wild type and explains a less pronounced allosteric modulation of norepinephrine binding at the E122L mutant. (**b**) Simulations snapshots of neutral AS408 at the E122L mutant illustrating the main conformations adopted by AS408. (**c**) In the simulations of neutral AS408 at the E122R mutant, AS408 adopts several conformations showing different interaction patterns. Most observed states have a hydrogen bond of AS408 to the backbone oxygen of V206$^{5.45}$ in common. (**d**) Simulations snapshots of neutral AS408 at the E122R mutant illustrating the main conformations adopted by AS408.

Supplementary Note: Synthetic Procedures

Synthesis of AS408 and analogues
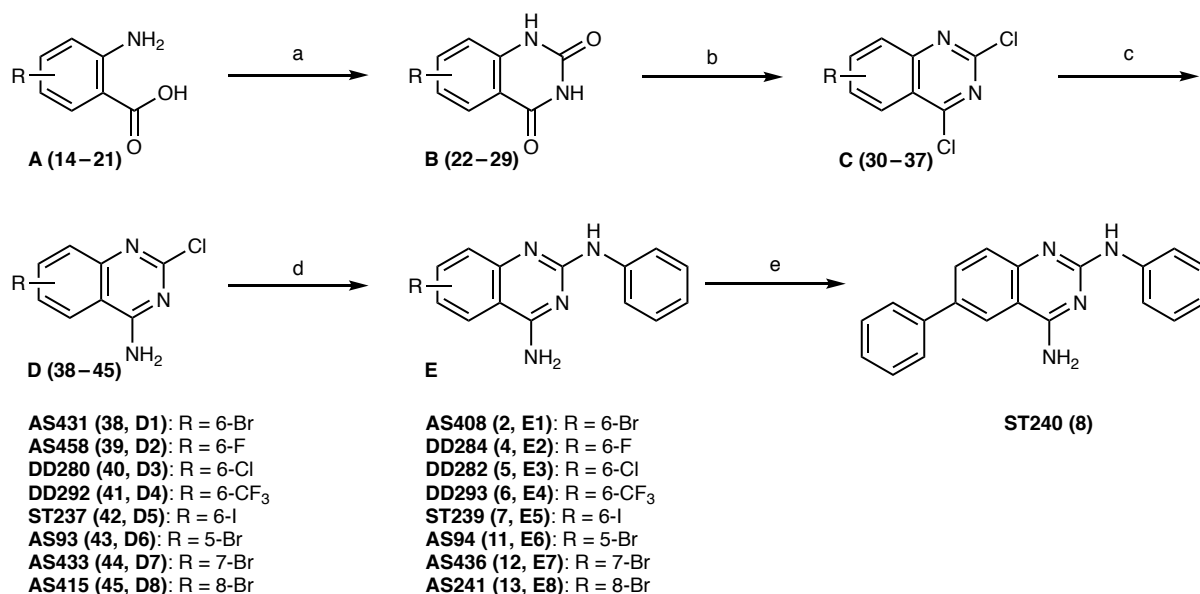
Scheme 1. a) urea, 150 °C, 16 h; b) POCl$_3$, PhN(Me)$_2$, 120 °C, 16 h; c) NH$_4$OH, THF, 2 h; d) aniline, EtOH, 80 °C, 16 h; e) **ST239**, PhB(OH)$_2$, Na$_2$CO$_3$, Pd(dppf)Cl$_2$, dioxane/H$_2$O, 80 °C, 3 h.

A series of phenylquinazoline-2,4-diamines (Scheme 1) was synthesized following a modified, previously described reaction sequence[3,4]. Starting from commercially available anthranilic acids of type **A** (**14 – 21**), cyclocondensation reaction with urea gave access to the bicyclic intermediates of type **B** (**22 – 29**). Phosphoryl oxychloride promoted chlorination of **B** (yielding **C** (**30 – 37**)), followed by a regioselective aminolysis gave the chloroquinazolin-4-amines **D** (**38 – 45**), which could be transformed into the test compounds of type **E** (**2, 4 – 7, 11 – 13**) by treatment with aniline in ethanol under reflux conditions. The biphenyl derivative **ST240** (**8**) was prepared by palladium assisted coupling of the aryliodide **ST239** (**7**) with phenylboronoic acid.

3   Althuis, T. H. & Hess, H. J. Synthesis and identification of the major metabolites of prazosin formed in dog and rat. *J Med Chem* **20**, 146-149, doi:10.1021/jm00211a031 (1977).

4   Zhang, L. *et al.* Synthesis and biological activities of quinazoline derivatives with ortho-phenol-quaternary ammonium salt groups. *Bioorg Med Chem* **15**, 6920-6926, doi:10.1016/j.bmc.2007.07.053 (2007).
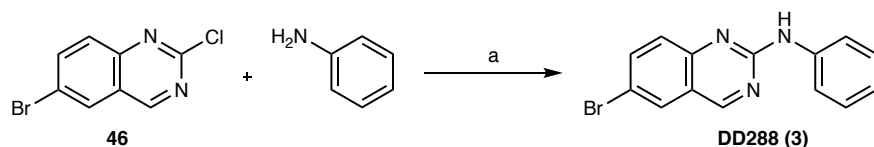
Scheme 2. a) EtOH, 80 °C, 6 h.

Compound **DD288** (**3**) was synthesized by treatment of commercially available 6-bromo-2-chloroquinazoline (**46**) with aniline.

General

All chemicals and solvents were purchased from Sigma Aldrich, Acros, Alfa Aesar, or Activate Scientific and were used without additional purification. Anhydrous solvents were of the highest commercially available grade and were stored over molecular sieves under a nitrogen atmosphere. The derivatives BRAC1, BRAC1-5 and BRAC1-23 were purchased. Flash chromatography was performed on Merck silica gel 60 (40 – 63 μm) as stationary phase under positive pressure of dry nitrogen gas. TLC analyses were performed using Merck 60 F254 aluminum plates in combination with UV detection (254 nm). HR-MS was run on an AB Sciex Triple TOF660 SCiex, source type ESI, or on a Bruker maXis MS in the laboratory of the Chair of Organic Chemistry, FAU, or on a Bruker maXis MS in the laboratory of the Chair of Bioinorganic Chemistry, FAU. Mass detection was conducted with a Bruker Esquire 2000 ion trap mass spectrometer using APCI or ESI ionization source or with Bruker amaZon SL mass spectrometer in combination with an Agilent 1100 or Dionex Ultimate 3000 UHPLC system. Analytical HPLC was conducted on an Agilent 1200 HPLC system employing a DAD detector and a ZORBAX ECLIPSE XDB-C8 (4.6 × 150 mm, 5 μm) column with the following binary solvent systems: System 1: eluent, methanol/0.1% aq. formic acid, starting from 10% methanol for 3 min to 100% in 15 min, 100% for 6 min to 10% in 3 min, then 10% for 3 min, flow rate 0.5 mL/min, λ = 210 or 254 nm; System 2: CH_3CN/0.1% aq. formic acid, from 10% CH_3CN for 3 min to 100% in 15 min, 100% for 6 min to 10% in 3 min, then 10% for 3 min, flow rate 0.5 mL/min, λ = 210 or 254 nm. Preparative HPLC was performed on an Agilent 1100 Preparative Series, using a ZORBAX ECLIPSE XDB-C8 PrepHT (21.5 x 150 mm, 5 μm, flow rate 10 mL/min) column with the solvent systems indicated. ^{1}H, and ^{13}C and DEPTQ NMR spectra were recorded on a Bruker

Avance 360, Avance 400 or a Bruker Avance 600 FT-NMR-Spectrometer. Chemical shifts were calculated as ppm relative to TMS (^{1}H) or solvent signal (^{13}C, DEPTQ) as internal standards.

## General procedure for the synthesis of the intermediates of type D

According to a modified, previously described reaction sequence[3], the compound of type **A** (1 eq.) was added in portions to heated, melted urea (10 eq.) and the mixture was stirred at 150 °C for 16 h. After cooling to room temperature, water was added and the mixture was sonicated for 30 min to get a finely dispersed precipitate, which was collected by filtration, washed several times with water and dried in vacuo. The obtained quinazoline-2,4(1*H*,3*H*)-dione of type **B** (1 eq.) was suspended in POCl$_3$ (~0.5 mL/mmol) at room temperature, and *N,N*-dimethylaniline (cat. amounts, 2-3 drops) was added. After the reaction mixture was stirred at 120 °C for 16 h, it was cooled to room temperature and poured carefully on ice. The formed precipitate of type **C** was collected by filtration, washed several times with water and dissolved in THF (2-3 mL/mmol). Aqueous ammonia (25%, $1-2$ mL/mmol) was added and the reaction mixture was stirred for 2 h at room temperature. After removal of THF under reduced pressure, the aqueous solution was lyophilized to obtain the 2-chloroquinazolin-4-amine of type **D**, which was used in the next step without further purification, otherwise it is indicated below.

6-Bromo-2-chloroquinazolin-4-amine (**AS431, 38**)
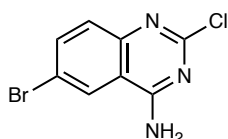
Reaction of 6-bromo-2,4-dichloroquinazoline (**C1**) and purification of the crude material by silica gel chromatography (CH$_2$Cl$_2$/MeOH, 30:1 v/v) resulted in **AS431** (185 mg, 0.72 mmol, 85%) as a light beige solid; ^{1}H NMR (600 MHz, DMSO-*d$_6$*) δ 8.54 (d, *J* = 2.1 Hz, 1H), 8.43 (br s, 2H), 7.93 (dd, *J* = 8.9, 2.2 Hz, 1H), 7.56 (d, *J* = 8.9 Hz, 1H); ^{13}C NMR (100 MHz, DMSO-*d$_6$*) δ 163.9, 158.1, 148.2, 137.3, 126.6, 123.7, 121.1, 114.5; ESI-MS *m/z* 257.9 [M+H]$^+$.

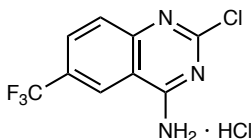*2-Chloro-6-fluoroquinazolin-4-amine x HCl* **(AS458, 39)**
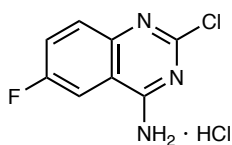
Reaction of 2-amino-5-fluorobenzoic acid (**A2**) resulted in **AS458** (490 mg, 2.09 mmol, 34% over 3 steps) as a light yellow solid, which was used in the next step without further purification; ^{1}H NMR (400 MHz, DMSO-d_6) δ 8.41 (br s, 2H), 8.17 (dd, J = 9.5, 2.5 Hz, 1H), 7.77 – 7.65 (m, 2H); ^{13}C NMR (100 MHz, DMSO-d_6) δ 163.3 (d, J = 3.9 Hz), 159.1 (d, J = 244.2 Hz), 156.7, 147.9, 129.3 (d, J = 8.6 Hz), 123.2 (d, J = 24.8 Hz), 113.6 (d, J = 9.1 Hz), 108.5 (d, J = 23.7 Hz); ESI-MS m/z 197.8 [M+H]$^+$.

2,6-Dichloroquinazolin-4-amine x HCl **(DD280, 40)**
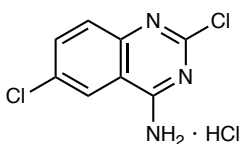
Reaction of 2-amino-5-chlorobenzoic acid (**A3**) resulted in **DD280** (334 mg, 1.56 mmol, 27% over 3 steps) as a light yellow solid, which was used in the next step without further purification; ^{1}H NMR (400 MHz, DMSO) δ 8.44 (s, 2H), 8.40 (d, J = 2.2 Hz, 1H), 7.83 (dd, J = 8.9, 2.2 Hz, 1H), 7.64 (d, J = 8.9 Hz, 1H); ^{13}C NMR (100 MHz, DMSO-$d6$) δ 162.8, 157.4, 149.5, 134.2, 129.9, 128.7, 123.2, 114.0; ESI-MS m/z 213.8 [M+H]$^+$.

*2-Chloro-6-(trifluoromethyl)quinazolin-4-amine x HCl* **(DD292, 41)**

Reaction of 2-amino-5-(trifluoromethyl)benzoic acid (**A4**) resulted in **DD292** (160 mg, 0.73 mmol, 30% over 3 steps) as raw dirty green solid, which was used in the next step without further purification; ESI-MS m/z 247.7 [M+H]$^+$.

*6-Iodo-2-chloroquinazolin-4-amine x HCl* **(ST237, 42)**
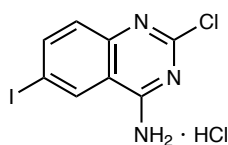
Reaction of 2-amino-5-iodobenzoic acid (**A5**) resulted in **ST237** (265 mg, 0.78 mmol, 26% over 3 steps) as a light yellow solid, which was used in the next step without further purification; ^{1}H NMR (400 MHz, DMSO-d_6) δ 8.67 (d, J = 1.9 Hz, 1H), 8.40 (br s, 2H), 8.05 (dd, J = 8.8, 1.9 Hz, 1H), 7.39 (d, J = 8.8 Hz, 1H); ^{13}C/DEPTQ NMR (400 MHz, DMSO-d_6) δ 162.4, 157.3, 150.0, 142.2, 132.4, 128.5, 114.9, 90.6; ESI-MS m/z 305.75 [M+H]$^+$.

5-Bromo-2-chloroquinazolin-4-amine x HCl **(AS93, 43)**
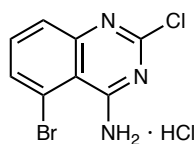
Reaction of 2-amino-6-bromobenzoic acid (**A6**) resulted in **AS93** (60 mg, 0.20 mmol, 56% over 3 steps) as a colorless solid, which was used in the next step without further purification; ^{1}H NMR (600 MHz, DMSO-d_6) δ 8.80 (br s, 1H), 7.93 (br s, 1H), 7.79 (dd, J = 7.3, 1.6 Hz, 1H), 7.68 – 7.61 (m, 2H); ^{13}C NMR (150 MHz, DMSO-d_6) δ 162.9, 156.9, 154.1, 134.7, 132.7, 127.6, 118.0, 112.3; ESI-MS m/z 257.7 [M+H]$^+$.

7-Bromo-2-chloroquinazolin-4-amine x HCl **(AS433, 44)**
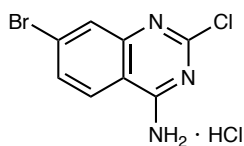
Reaction of 2-amino-4-bromobenzoic acid (**A7**) resulted in **AS433** (780 mg, 2.64 mmol, 65% over 3 steps) as a light beige solid, which was used in the next step without further purification; ^{1}H NMR (400 MHz, DMSO-d_6) δ 8.62 (br s, 1H), 8.46 (br s, 1H), 8.27 (d, J = 8.8 Hz, 1H), 7.83 (d, J = 1.9 Hz, 1H), 7.69 (dd, J = 8.8, 2.0 Hz, 1H); ^{13}C NMR (100 MHz, DMSO-d_6) δ 163.5, 158.1, 151.9, 128.9, 128.6, 127.6, 126.2, 112.1; ESI-MS m/z 257.9 [M+H]$^+$.

*8-Bromo-2-chloroquinazolin-4-amine* **(AS415, 45)**
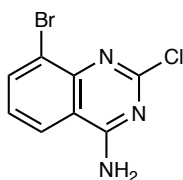
Reaction of 2-amino-3-bromobenzoic acid (**A8**) and purification of the crude material by silica gel chromatography (CH$_2$Cl$_2$/MeOH, 30:1 v/v) resulted in **AS415** (120 mg, 0.47 mmol, 45% over 3 steps) as a colorless solid; ^{1}H NMR (600 MHz, DMSO-d_6) δ 8.53 (br s, 2H), 8.24 (dd, J = 8.2, 1.0 Hz, 1H), 8.14 (dd, J = 7.6, 1.0 Hz, 1H), 7.43 (t, J = 7.9 Hz, 1H); ^{13}C NMR (150 MHz, DMSO-d_6) δ 163.9, 158.1, 148.2, 137.3, 126.6, 123.7, 121.1, 114.5; ESI-MS m/z 257.8 [M+H]$^+$.

General procedure for the synthesis of compounds of type E

According to a modified, previously described reaction sequence[4], aniline (4 eq.) was added to a solution of the 2-chloroquinazolin-4-amine of type **D** (1 eq.) in anhydrous ethanol (~20 mL/mmol) in a pressure tube and the reaction mixture was stirred at 80 °C for 16 h. The solvent was evaporated, and the crude material was treated with saturated, aqueous NaHCO$_3$ and extracted three times with CH$_2$Cl$_2$. The combined organic phases were dried (MgSO$_4$) and the solvent was evaporated. The obtained residue was purified as indicated below.

6-Bromo-N^2-phenylquinazoline-2,4-diamine x HCOOH (**AS408, 2**)
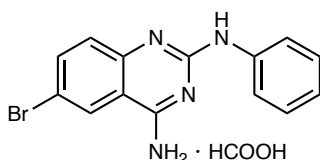
Intermediate **AS431** was reacted according to general procedure. The crude material was purified by preparative HPLC (acetonitrile in 0.1% aq. HCOOH, 5% to 95%) to yield **AS408** as a light beige solid (25.0 mg, 90%); ^{1}H NMR (600 MHz, DMSO-d_6) δ 9.05 (s, 1H), 8.35 (d, J = 2.2 Hz, 1H), 8.14 (br s, 1H), 7.95 – 7.86 (m, 2H), 7.69 (dd, J = 8.9, 2.2 Hz, 1H), 7.57 (br s, 2H), 7.34 (d, J = 8.9 Hz, 1H), 7.30 – 7.20 (m, 2H), 6.97 – 6.83 (m, 1H); ^{13}C NMR (150 MHz, DMSO-d_6) δ 161.7, 157.9, 150.9, 141.6, 136.0, 128.7 (2C), 127.9, 126.4, 121.1, 119.2 (2C), 113.3, 113.0; ESI-MS m/z 315.0 [M+H]$^+$; HRMS-ESI (m/z) [M+H]+: calcd. for C$_{14}$H$_{11}$BrN$_4$: 315.0240, found: 315.0238; HPLC: System 1: t_R = 16.0 min, purity 97%, System 2: t_R = 13.7 min, purity 99%.

6-Bromo-N-phenylquinazolin-2-amine **(DD288, 3)**[5]
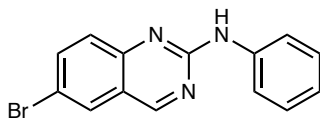
90.0 μL Aniline (4 eq., 0.99 mmol) were added to a solution of 60.0 mg of 6-bromo-2-chloroquinazoline (1 eq., 0.25 mmol) in anhydrous ethanol (4 mL) in a pressure tube and the reaction mixture was stirred at 80 °C for 6 h. The solvent was evaporated and the crude material was purified by silica gel flash chromatography (EtOAc/hexane, 3:1 v/v) giving **DD288** as a yellow solid (72.4 mg, 98%); ^{1}H NMR (600 MHz, CDCl$_3$) δ 9.02 – 8.97 (m, 1H), 7.86 (d, J = 2.2 Hz, 1H), 7.82 – 7.77 (m, 3H), 7.62 (d, J = 8.9 Hz, 1H), 7.46 (br s, 1H), 7.40 – 7.36 (m, 2H), 7.09 (tt, J = 7.5, 1.0 Hz, 1H); ^{13}C NMR (150 MHz, CDCl$_3$) δ 160.8, 156.9, 150.3, 139.2, 137.6, 129.4, 129.0, 128.2 (2C), 122.9, 121.8, 119.2 (2C), 116.5; ESI-MS m/z 299.9 [M+H]$^+$; HRMS-ESI (m/z) [M+H]+: calcd. for C$_{14}$H$_{11}$BrN$_3$: 300.0131, found: 300.0133; HPLC: System 1: t$_R$ = 21.5 min, purity 99%, System 2: t$_R$ = 20.3 min, purity 99%.

5   DiMauro, E. F. *et al.* Discovery of aminoquinazolines as potent, orally bioavailable inhibitors of Lck: synthesis, SAR, and in vivo anti-inflammatory activity. *J Med Chem* **49**, 5671-5686, doi:10.1021/jm0605482 (2006).

*6-Fluoro-N^2-phenylquinazoline-2,4-diamine x HCOOH* **(DD284, 4)**
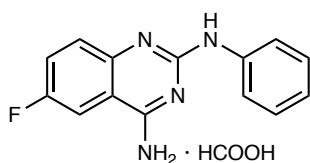
Intermediate **AS458** was reacted according to general procedure. The crude material was purified by preparative HPLC (acetonitrile in 0.1% aq. HCOOH, 15% to 70%) to give **DD284** as a white solid (55.0 mg, 85%); ^{1}H NMR (400 MHz, DMSO-d_6) δ 9.00 (s, 1H), 8.18 (br s, 1H), 7.99 – 7.87 (m, 3H), 7.61 – 7.40 (m, 4H), 7.25 (t, J = 7.9 Hz, 2H), 6.89 (t, J = 7.3 Hz, 1H); ^{13}C NMR (100 MHz, DMSO-d_6) δ 161.8 (d, J = 3.6 Hz), 157.0, 156.7 (d, J = 240.4 Hz), 148.4, 141.4, 128.3 (2C), 127.4 (d, J = 7.9 Hz), 121.9 (d, J = 24.4 Hz), 120.5, 118.6 (2C), 111.0 (d, J = 8.4 Hz), 108.0 (d, J = 22.9 Hz); ESI-MS m/z 255.0 [M+H]$^+$; HRMS-ESI (m/z) [M+H]$^+$: calcd. for

$C_{14}H_{12}FN_4$: 255.1041, found: 255.1044; HPLC: System 1: t_R = 14.5 min, purity 98%, System 2: t_R = 12.6 min, purity 99%.

6-Chloro-N^2-phenylquinazoline-2,4-diamine x HCOOH (DD282, 5)
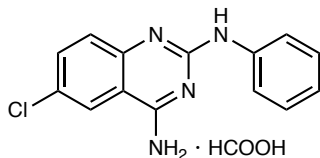

Intermediate **DD280** was reacted and the crude material was purified by preparative HPLC (acetonitrile in 0.1% aq. HCOOH, 35% to 90%) to give **DD282** as a white solid (63.8 mg, 84%); ^{1}H NMR (400 MHz, DMSO-d_6) δ 9.05 (s, 1H), 8.22 (d, J = 2.3 Hz, 1H), 8.17 (br s, 1H), 7.91 (d, J = 7.8 Hz, 2H), 7.69 – 7.49 (br s, 1H), 7.59 (dd, J = 8.9, 2.3 Hz, 2H), 7.41 (d, J = 8.9 Hz, 1H), 7.25 (t, J = 7.9 Hz, 2H), 6.90 (t, J = 7.3 Hz, 1H), ^{13}C NMR (100 MHz, DMSO-d_6) δ 161.4, 157.5, 150.3, 141.3, 133.1, 128.3 (2C), 127.3, 125.1, 122.9, 120.8, 118.8 (2C), 112.0; ESI-MS m/z 270.9 [M+H]$^+$; HRMS-ESI (m/z) [M+H]+: calcd. for $C_{14}H_{12}ClN_4$: 271.0745, found: 271.0747; HPLC: System 1: t_R = 15.3 min, purity 98%, System 2: t_R = 13.1 min, purity 98%.

## 6-Trifluoromethyl-N^2-phenylquinazoline-2,4-diamine x HCOOH (DD293, 6)
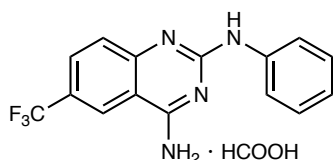
Intermediate **DD292** was reacted and the crude material was purified by preparative HPLC (acetonitrile in 0.1% aq. HCOOH, 15% to 95%) to give **DD293** as a yellowish white solid (9.80 mg,13%); ^{1}H NMR (600 MHz, DMSO-d_6) δ 9.22 (s, 1H), 8.56 (s, 1H), 7.92 (d, J = 7.7 Hz, 2H), 7.81 (dd, J = 8.8, 1.9 Hz, 1H), 7.77 (br s, 2H), 7.51 (d, J = 8.7 Hz, 1H), 7.30 – 7.22 (m, 2H), 6.95 – 6.90 (m, 1H); ^{13}C NMR (150 MHz, DMSO-d_6) δ 162.3, 158.6, 154.0, 141.0, 128.4 (q, J = 4 Hz), 128.3 (2C), 126.2, 124.6 (q, J = 271.5 Hz), 122.2 (q, J = 4 Hz), 121.1 (q, J = 31.7 Hz), 121.0, 119.1 (2C), 110.4; ESI-MS m/z 304.9 [M+H]$^+$; HRMS-ESI (m/z) [M+H]+: calcd. for $C_{15}H_{12}F_3N_4$: 305.1009, found: 305.1010; HPLC: System 1: t_R = 16.1 min, purity 96%, System 2: t_R = 13.7 min, purity 97%.

6-Iodo-N²-phenylquinazoline-2,4-diamine x HCl **(ST239, 7)**
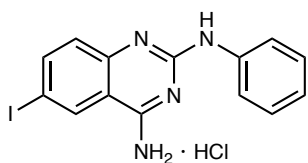
ST237 (100 mg, 0.33 mmol) and aniline (120 μL, 1.31 mmol) in EtOH (6.5 mL) were heated for 13 h at 80°C. The pure product crystallized out of the reaction. After cooling down to room temperature, the product was isolated by suction filtration, washed with cold EtOH to yield a light yellow solid. The filtrate was concentrated and further product crystallized out of the solution to yield **ST239** as a light yellow solid (52.0 mg, 0.13 mmol, 40%); ^{1}H NMR (400 MHz, DMSO-d_6) δ 12.87 (br s, 1H), 10.52 (s, 1H), 9.34 (br s, 1H), 9.23 (br s, 1H), 8.73 (d, J = 1.8 Hz, 1H), 8.10 (dd, J = 1.8, 8.8 Hz, 1H), 7.60 – 7.66 (m, 2H), 7.37 – 7.44 (m, 2H), 7.34 (d, J = 8.8 Hz, 1H), 7.16 – 7.25 (m, 1H); ^{13}C/DEPTQ NMR (400 MHz, DMSO-d_6) δ 161.8, 151.7, 143.6, 138.8, 136.9, 133.2, 129.1 (2C), 124.9, 122.1, 119.4 (2C), 111.7, 88.4; ESI-MS *m/z* 362.9 [M+H]$^+$; HRMS-ESI (m/z) [M+H]+: calcd. for C$_{14}$H$_{12}$IN$_4$: 363.0101, found: 363.0101; HPLC: System 1: t_R = 15.7 min, purity 99%, System 2: t_R = 12.1 min, purity 99%.

N²,6-Diphenylquinazoline-2,4-diamine x TFA **(ST240, 8)**
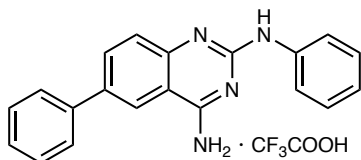
Phenylboronic acid (25.6 mg, 0.21 mmol), Na$_2$CO$_3$ (89.0 mg, 0.84 mmol) and Pd(dppf)Cl$_2$ (15.4 mg, 0.021 mmol) were dissolved in a dioxane/H$_2$O mixture (4:1, 5 mL) in a microwave vial. **ST239** (38.0 mg, 0.11 mmol) was added to the mixture and the reaction was heated under argon atmosphere at 80 °C for 3 h. After the reaction has cooled to room temperature, water was added, and the aqueous phase was extracted with ethyl acetate three times. The combined organic layers were washed with brine, dried (Na$_2$SO$_4$) and evaporated. The crude product was purified by preparative HPLC (acetonitrile in 0.1% aq. trifluoroacetic acid, 5% to 60%) to yield **ST240** as a white solid (21.0 mg, 47%); ^{1}H NMR (400 MHz, DMSO-d_6) δ 13.51 (br s, 1H), 10.79 (s, 1H), 9.32 (br s, 1H), 9.12 (br s, 1H), 8.63 (d, J = 1.8 Hz, 1H), 8.20 (dd, J = 1.8, 8.7 Hz, 1H), 7.77 – 7.84 (m, 2H), 7.67 – 7.74 (m, 2H), 7.59 (d, J = 8.7

Hz, 1H), 7.49 – 7.56 (m, 2H), 7.38 – 7.46 (m, 3H), 7.15 – 7.23 (m, 1H); ^{13}C/DEPTQ NMR (400 MHz, DMSO-d_6) δ 163.1, 159.0, 158.7, 152.0, 138.3, 137.5, 136.1, 133.9, 129.1 (2C), 129.0 (2C), 128.0, 126.6 (2C), 124.5, 122.3, 121.8, 118.3, 110.2; ESI-MS m/z 313.0 [M+H]$^+$; HRMS-ESI (m/z) [M+H]+: calcd. for $C_{20}H_{17}N_4$: 313.1448, found: 313.1455; HPLC: System 1: t_R = 17.0 min, purity 99%, System 2: t_R = 13.2 min, purity 99%.

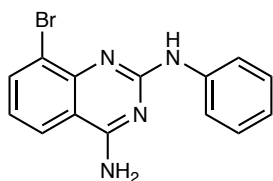*5-Bromo-N^2-phenylquinazoline-2,4-diamine* **(AS94, 11)**
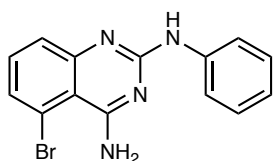
Intermediate **AS93** was reacted and the crude material was purified by silica gel chromatography (CH_2Cl_2/MeOH, 30:1 v/v) to obtain **AS94** as a light beige solid (30.3 mg, 58%); ^{1}H NMR (600 MHz, DMSO-d_6) δ 9.13 (s, 1H), 7.95 – 7.85 (m, 2H), 7.55 (br s, 2H), 7.45 – 7.38 (m, 3H), 7.29 – 7.22 (m, 2H), 6.95 – 6.88 (m, 1H); ^{13}C NMR (150 MHz, DMSO-d_6) δ 161.4, 156.9, 155.1, 141.5, 133.6, 128.8 (2C), 128.1, 126.4, 121.3, 119.3 (2C), 118.0, 110.2; ESI-MS m/z 315.4 [M+H]$^+$; HRMS-ESI (m/z) [M+H]+: calcd. for $C_{14}H_{12}BrN_4$: 315.0240, found: 315.0251; HPLC: System 1: t_R = 15.4 min, purity 98%, System 2: t_R = 14.4 min, purity 98%.

7-Bromo-N^2-phenylquinazoline-2,4-diamine x HCOOH **(AS436, 12)**
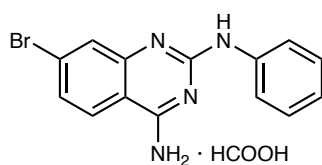
Intermediate **AS433** was reacted and the crude material was purified by preparative HPLC (acetonitrile in 0.1% aq. HCOOH, 5% to 95%) to give **AS436** as a light beige solid (32.5 mg, 76%); ^{1}H NMR (600 MHz, DMSO-d_6) δ 9.12 (s, 1H), 8.14 (s, 1H), 8.03 (d, J = 8.6 Hz, 1H), 7.90 (d, J = 7.9 Hz, 2H), 7.63 (br s, J = 36.4 Hz, 2H), 7.57 (br s, 1H), 7.30 (d, J = 8.6 Hz, 1H), 7.25 (t, J = 7.8 Hz, 2H), 6.91 (t, J = 7.3 Hz, 1H); ^{13}C NMR (100 MHz, DMSO-d_6) δ 163.5, 162.5, 158.2, 153.2, 141.5, 128.7 (2C), 127.3, 126.9, 126.2, 124.5, 121.3, 119.4 (2C); ESI-MS m/z 315.0 [M+H]$^+$; HPLC: System 1: t_R = 16.3 min, purity 99%, System 2: t_R = 16.6 min, purity 99%.

8-Bromo-N²-phenylquinazoline-2,4-diamine **(AS241, 13)**

Intermediate **AS415** was reacted and the crude material was purified by silica gel chromatography (CH$_2$Cl$_2$/MeOH, 30:1 v/v) to give **AS241** as a light beige solid (41.1 mg, 84%); ^{1}H NMR (600 MHz, DMSO-d_6) δ 9.13 (s, 1H), 8.14 (d, J = 8.0 Hz, 2H), 8.11 (dd, J = 8.1, 0.9 Hz, 1H), 7.96 (dd, J = 7.6, 1.0 Hz, 1H), 7.59 (br s, 2H), 7.27 (t, J = 7.9 Hz, 2H), 7.09 (t, J = 7.8 Hz, 1H), 6.92 (t, J = 7.3 Hz, 1H); ^{13}C NMR (90 MHz, DMSO-d_6) δ 162.3, 157.3, 149.0, 141.2, 135.9, 128.3 (2C), 123.3, 121.9, 120.7, 120.1, 118.7 (2C), 112.8; ESI-MS *m/z* 314.7 [M+H]$^+$; HRMS-ESI (m/z) [M+H]+: calcd. for C$_{14}$H$_{12}$BrN$_4$: 315.0240, found: 315.0244; HPLC: System 1: t_R = 16.0 min, purity 99%, System 2: t_R = 14.0 min, purity 99%.